Geophysical Structure of The Troodos Ophiolite from Downhole Logging

M.H. SALISBURY[1], N.I. CHRISTENSEN[2], F.J. VINE[3], G.C. SMITH[3] AND S. ELEFTHERIOU[4]

[1]Centre for Marine Geology, Dalhousie University Halifax, Nova Scotia, Canada B3H 3J5
[2]Department of Earth and Atmospheric Sciences Purdue University, West Lafayette, IN., U.S.A. 47907
[3]School of Environmental Sciences University of East Anglia, Norwich United Kingdom NR4 7TJ
[4] Geological Survey Department, Nicosia, Cyprus

Salisbury, M.H., Christensen, N.I., Vine, F.J., Smith G.C., Eleftheriou, S., Geophysical structure of the Troodos ophiolite from downhole logging in *Cyprus Crustal Study Project: Initial Report, Hole CY-4, ed. I.L. Gibson, J. Malpas, P.T. Robinson and C. Xenophontos; Geological Survey of Canada, Paper 88-9, p. 331-349, 1989.*

Abstract

Velocity (Vp and Vs), density, porosity, natural gamma, resistivity, total magnetic field and magnetic susceptibility logs demonstrate that the Troodos ophiolite complex is geophysically similar to the oceanic crust. Insitu velocities (Vp) range from 3.2-3.5 km/s in the pillow basalts (Layer 2A) and then increase gradually through the pillow basalt/dike transition and the sheeted dikes (Layer 2B) to classic Layer 3 velocities (6.7-6.9 km/s) in the gabbros while Vs averages 2.1 km/s in the pillow basalts and rises to values of 3.2-3.5 km/s in the gabbros. In the pyroxenites, Vp increases only slightly (to 7.0 km/s) but Vs rises to 4.0 km/s. The porosity and natural gamma radiation decrease from averages of 20% and 30 API units, respectively, in the pillow basalts to negligible values in the gabbros, while the formation density and resistivity increase from 2.2 to 2.95 g/cm^3 and from 10 to 20K-50K ohm-m over the same interval, suggesting that seawater penetrates no deeper than the base of the dikes. Aside from Vs, the only property which changes at the gabbro/pyroxenite boundary is density, which increases abruptly to 3.1 g/cm^3 The magnetic susceptibility increases steadily from 0.5×10^{-3} S.I. units in the pillow basalts to 4×10^{-3} units at the 50% dike/50% gabbro transition, below which it decreases abruptly to 0.5×10^{-3} units. Since resistivity increases by an order of magnitude at the same depth and Vp increases rapidly from 5.75 to 6.4 km/s at this depth and then increases steadily to 6.8 km/s within the next few hundred meters, we interpret the dike/gabbro transition as the Layer 2/3 boundary of the oceanic crust.

Résumé

Les enregistrements continus, des vitesses séismiques Vp et Vs, densité, porosité, radioactivité naturelle, résistivité, champ magnétique total, susceptibilitè magnétique, constituent un ensemble géophysique similaire à celui de la croûte océanique. Les vitesses Vp mesurées in situ varient de 3.2 à 3.5 km/s dans les basaltes coussinées (Couche 2A) et augmentent progressivement vers la zone de transition de basaltes coussinés/dykes et le complexe filonien (Couche 2B) jusqu'à des vitesses caractéristiques de la Couche 3 (6.7-6.9 km/s) dans les gabbros. Parallèlement les vitesses moyennes Vs sont de l'ordre de 2.1 km/s dans les basaltes coussinés et croissent à 3.2-3.5 km/s dans les gabbros. Dans les pyroxénites les vitesses Vp augmentent légèrement à 7.0 km/s alors que les vitesses Vs s'accroissent à 4.0 km/s. La porosité et la radiation gamma naturelle décroissent respectivement depuis 20% et 30 unités API en moyenne dans les basaltes coussinés à des valeurs négligeables dans les gabbros. Dans le même intervalle, la densité et la résistivité augmentent respectivement de 2.2 à 2.95 g/cm^3 et de 10 à 20K-50K ohm-m, suggérant une pénétration maximale de l'eau de mer jusqu'à la base des dykes. En plus des vitesses Vs qui varient à l'interface gabbros/pyroxénites, la densité augmente brusquement à 3.1 g/cm^3. La susceptibilité magnétique croit continuellement de 0.5×10^{-3} unités S.I. dans les basaltes coussinés à 4×10^{-3} unités à la transition 50% dyke/50% gabbro. Sous cette zone la susceptibilité décroit brusquement à 0.5×10^{-3} unités. Puisque la résistivité augmente d'un ordre de grandeur à la même profondeur et que Vp s'accroit rapidement de 5.75 à 6.4 km/s et alors progressivement à 6.8 km/s à l'intérieur des quelques centaines de mètres suivants, nous interprétons la transition dykes-gabbros comme étant la limite des couches 2 et 3 de la croûte océanique.

INTRODUCTION

Since it was first proposed that the rock assemblages found in ophiolites represent fragments of oceanic crust tectonically emplaced on land, numerous investigations have been undertaken in these complexes to determine the validity of the hypothesis, or assuming it to be true, to determine the nature of oceanic crust. While hundreds of ophiolites have been identified and several dozen studied in detail (see Coleman, 1977, for review), the Troodos complex, which was first identified as an ophiolite in 1968 by Gass, remains one of the most extensively studied and convincing (e.g. Moores and Vine, 1971). While the exact provenance of the ophiolites remains uncertain - the presence of andesitic basalts and boninites in the Troodos extrusives suggests formation in a suprasubduction zone environment (Miyashiro, 1973; Robinson et al., 1983) - the presence of sheeted dikes, pillow basalts, massive sulphide deposits and fossilized smokers leaves no doubt that they formed in a submarine environment and represent, if not typical ocean crust, at least one of its variants. The recent discovery of dikes at a sub-basement depth of 500 m in two DSDP holes (418A and 504B; Leg 51-53 Shipboard Scientific Parties, 1980; Shipboard Scientific Party, 1985) and sheeted dikes at about 800 m in hole 504B lends further support to the hypothesis and suggests that in many key respects, ophiolites and ocean crust are indistinguishable.

Although the relative structural simplicity of the Troodos ophiolite has made it possible to determine the overall structure and stratigraphy of the complex, the discontinuous nature of the outcrops and the depth of weathering have made it difficult to determine important geochemical, magmatic and structural relationships with certainty. For example, it was unknown whether the extrusive and intrusive parts of any given vertical section were co-magmatic or whether the intrusives showed cryptic variation. Similarly, it was impossible to reconstruct a geophysical section through the complex based on hand samples because the physical properties of surface samples are strongly affected by alteration and because cracks, which strongly influence formation properties, are difficult to sample.

To address these questions and to determine the three-dimensional structure of the complex, the International Crustal Research Drilling Group (ICRDG) drilled an array of holes along a NE-SW transect across the northern flank of the ophiolite (Table 1; Figures 1 and 2). Since the complex is exposed in a broad anticline, with ultramafics and gabbros at the core, sheeted diabase dikes at higher levels and pillow basalts along the margins, the holes could be stacked to give a nearly complete cross-section through the crust (Figure 3).

TABLE 1: ICRDG Drillholes in the Troodos Ophiolite.

Hole	Coordinates	Penetration (m)	Logged Interval (m)	Crustal Level	Lithology	Depth[1] Range (m)
CY-1	35°02'54"N	485	-	Extrusives	Upper pillow basalts	0-300
	33°10'46"E				Lower pillow basalts	300-485
CY-2	35°02'43"N	226	-	Extrusives	Lower pillow basalts	0-226
	33°08'48"E				Hydrothermal stockwork	0-97
CY-2A	35°02'40"N	689	-	Extrusives	Lower pillow basalts	0-280
	33°08'55"E				Hydrothermal stockwork	154-297
					Basal group	280-689
CY-1A	35°02'10"N	701	-	Extrusives	Lower pillow basalts	0-200
	33°10'29"E				Basal group	200-701
CY-4	34°54'06"N	2263	0-2080	Plutonic	Lower sheeted dikes	0-675
	33°05'38"E				Massive gabbros	675-1330
					Cumulate gabbros	330-1740
					Cumulate ultramafics	1740-2263

(1) Based on petrology.

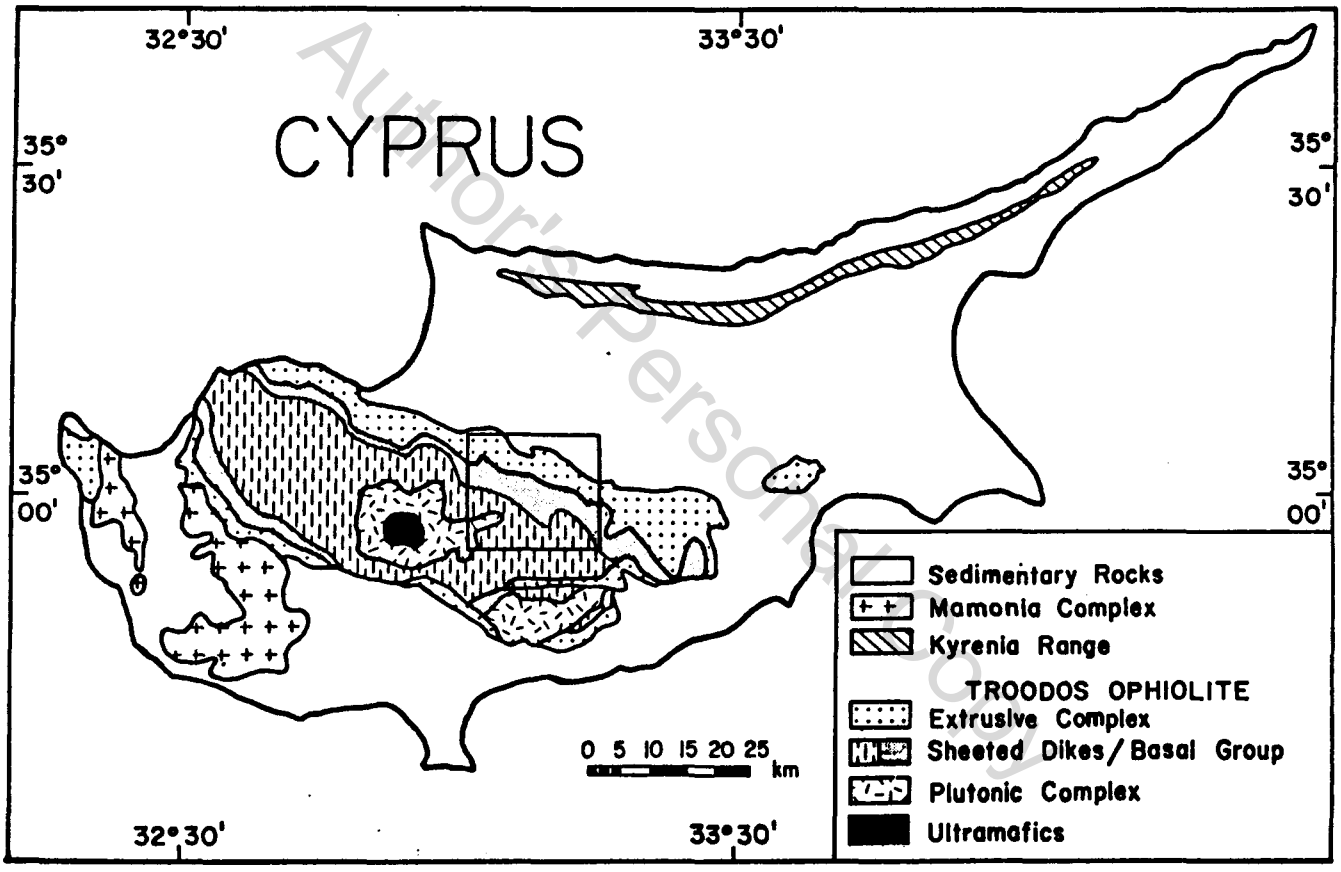

Figure 1: Geological map of Cyprus. Rectangle indicates area shown in Figure 2.

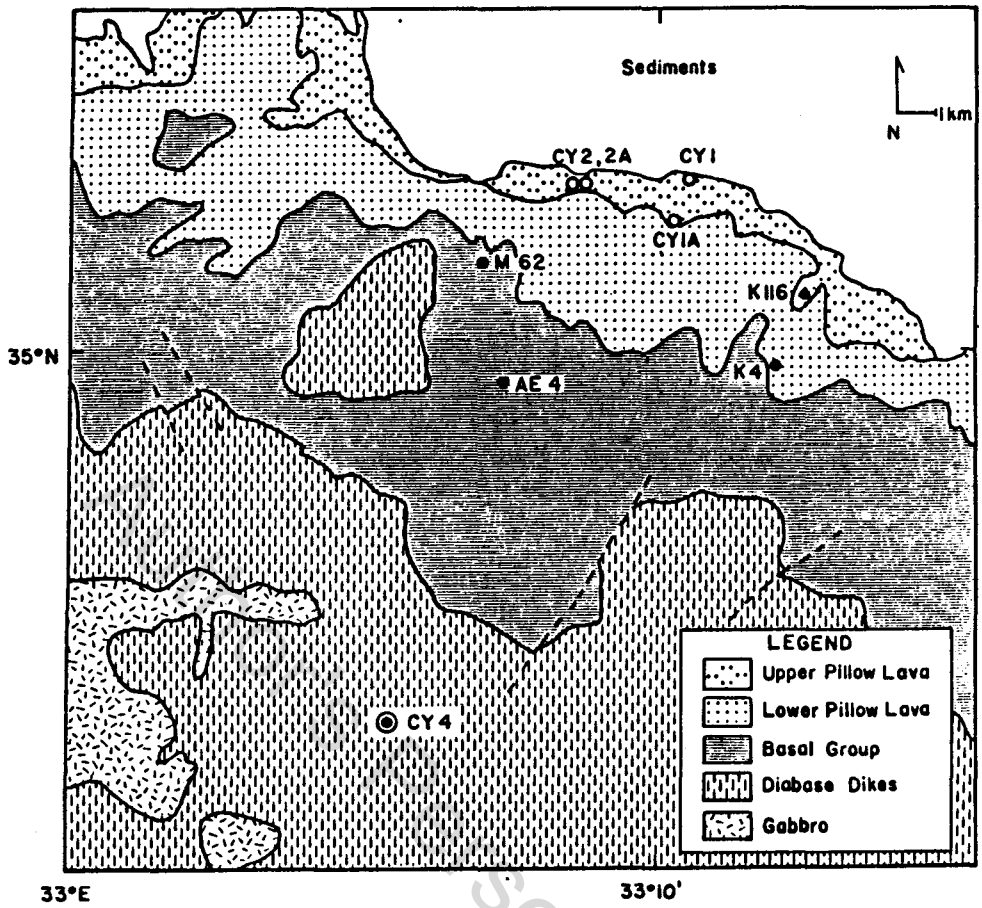

Figure 2: Holes drilled in Troodos ophiolite by the ICRDG (open circles), BRGM and Hellenic Mining. Logged holes indicated by filled circles.

From the inception of the project, it was recognized that the holes drilled through the Troodos ophiolite would provide an unparalled opportunity to determine the geophysical properties of oceanic crust by logging. Not only is the section virtually complete, but below the thin zone of surficial weathering described by field geologists, the alteration is submarine in origin (Gillis, 1986). Furthermore, the water table lies within a few metres of the surface, ensuring that conditions of water saturation are similar to those in the seafloor. Thus the present-day ophiolite only differs from its marine equivalents in terms of pore water salinity (salt water has been replaced by brackish water), effective confining pressure (the plutonic section has suffered a 0.5 to 1.0 kbar decompression due to uplift and erosion), temperature and crack density (new cracks were probably introduced during emplacement).

LOGGING OPERATIONS

To take advantage of this opportunity, a major downhole logging program was conducted in Cyprus during the summer of 1984 and again in the winter of 1985 using slimhole equipment supplied by BPB Instruments, Ltd. The logging suite (Table 2) consisted of eight separate tools selected to measure borehole temperature and diameter, natural gamma radiation, formation density and porosity, resistivity, compressional (Vp) and shear (Vs) wave velocity, magnetic field strength and magnetic susceptibility. The surface equipment consisted of a generator and a logging truck housing the power and control panels for each tool, recording equipment, a logging winch and calibration standards. The data from each tool was transmitted to the surface in analog form, then digitized and recorded for computer processing. Hard copies were made of the analog data for field interpretation.

TABLE 2: BPB Tools Used During Cyprus Logging Operations.

Tool	Measurement	Remarks
TT1	Temperature	Thermistor probe
DD3	Caliper	Single arm
	Natural γ	NaI/PMT sensor
	γ density	Borehole-compensated (2 channel)
NN1	Natural γ	NaI/PMT sensor
	Neutron porosity	Borehole-compensated (2 channel)
RO1	Resistivity	3-electrode laterolog
MS1	V_p	Multichannel sonic (4 channel)
Shear wave	V_s	Clamped; full wave
Magnetometer	Field strength	3-axis flux gate
Susceptibility	Magnetic susceptibility	Induction tool

Tool Descriptions

Temperature (TT1).

The simplest tool deployed was a temperature probe consisting of a thermistor in a cage mounted at the base of a 1.5 m long x 3.8 cm (1-1/2") diameter pressure housing. The tool was rated to 100°C and could operate in either the absolute or temperature differential modes with sensitivities of 0.1 and 0.001°C, respectively.

Gamma density (DD3).

The γ density tool was a combination caliper/natural gamma density tool in a 3.5 m long x 4.8 cm (1-7/8") diameter housing. The caliper consisted of a single arm electromechanical device which was retracted while lowering, but could be extended out to 12" while logging, causing the tool to be excentralized and providing a continuous record of borehole diameter.

The natural γ tool employs an uncollimated NaI crystal coupled to a photo-multiplier tube to measure total natural γ radiation. The tool provides an indirect measure of the U, K and Th content of the formation within 6" of the borehole wall (the average penetration of gamma rays in basalt) but cannot be used to determine their relative abundances.

The γ density tool is a dual-spaced, borehole-compensated tool consisting of a collimated, Caesium 137 sidewall source at the base of the tool and two NaI gamma ray sensors spaced 15 and 40 cm, respectively, above the source. The tool uses Compton scattering of gamma rays to determine the electron density and thus, the bulk density, of the formation within a foot of the source. The tool design allows the formation density to be determined accurately in irregular, water-filled boreholes up to 8" in diameter and qualitatively in holes from 8 to 12" in diameter. Since high formation densities were anticipated, the tool was equipped with a high energy (150 mCi) source to increase the gamma ray count and thus, the density range of the tool.

Neutron porosity (NN1).

The neutron porosity tool was a combination neutron porosity/natural gamma tool in a 2.5 m long x 3.8 cm (1-1/2") diameter housing. The natural γ sensor was the same as that used in the density tool and was used for correlation between logs.

The neutron porosity tool, like the density tool, is a dual-spaced, borehole-compensated tool designed for use in irregular, water-filled boreholes up to 12" in diameter. Unlike the density tool, however, the neutron tool is neither clamped nor centralized. The tool consists of a 1 Ci, Am 241/Be uncollimated source at the base of the tool and two thermal neutron detectors located 25 and 45 cm, respectively, above the source. The porosity of the formation is measured by determining the ability of the formation to slow high energy neutrons. Since the energy loss is greatest for collisions between particles of equal mass, the number of low energy (thermal) neutrons reaching the detectors is related to the hydrogen content of the formation within one foot of the source. Since the hydrogen resides largely in water, the tool provides a measure of the water content or porosity of the formation. The tool works best in fresh water because Cl and B also moderate the neutron flux (although to a lesser degree).

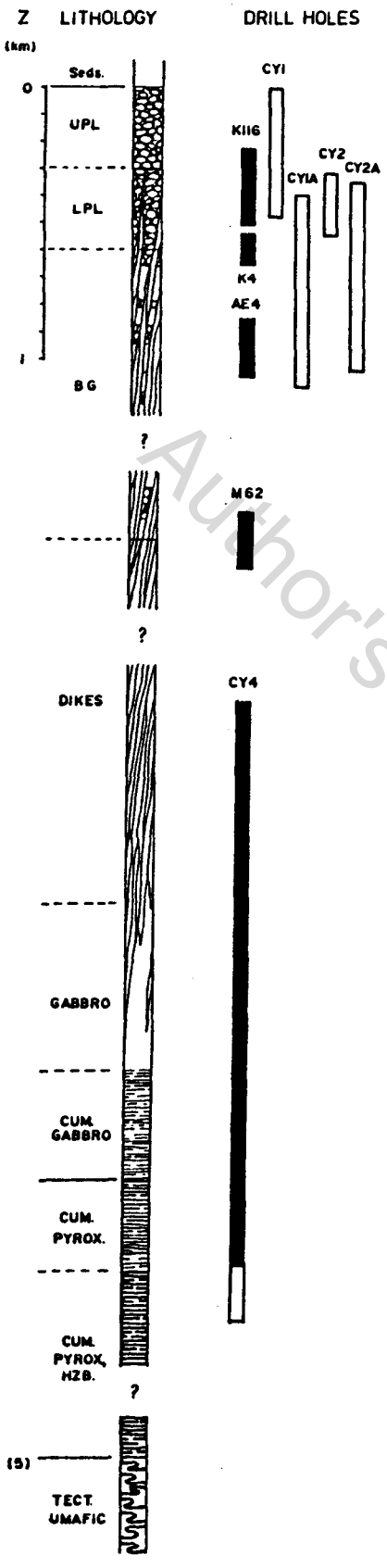

Resistivity (RO1).

The resistivity, or focussed electric sonde consists of a current electrode and two guard electrodes in a housing which measures 2.8 m long by 3.8 cm (1-1/2") in diameter. The tool measures formation resistivity as a function of depth by transmitting a constant current into the formation in the form of a thin, horizontal sheet and monitoring the voltage between an electrode located in the tool and a second electrode in a bridle 40 feet above the sonde. The tool can operate in fluid-filled holes up to 10" in diameter but works best in holes less than 8" in diameter. The depth of penetration depends on formation conditions, but often exceeds 1 m.

Compressional wave velocity (MS1).

Compressional wave velocities were measured using a multichannel sonic tool containing a ceramic transducer and four receivers spaced 60, 80, 100 and 120 cm, respectively, below the transmitter in a rigid housing measuring 3.4 m long by 6.5 cm (2-1/2") in diameter (including centralizers). Velocities were determined for different path lengths through the borehole wall by comparing the differences in first arrival times for different receiver pairs. The long (60 cm) path is felt to minimize the effects of rugosity and to provide the best average formation velocity while the short (20 cm) paths give fracture locations and the best bed resolution. The tool is designed to operate in water-filled boreholes up to 10" in diameter. Integrated travel times were computed from the velocity vs depth data after the completion of logging.

Shear wave velocity.

Shear wave velocities were determined using a prototype full wave sonic tool which was clamped against the borehole wall at selected depths, generally 10 m apart. The tool, which was 3 m long and 6.5 cm (2-1/2") in diameter has a rigid upper housing with an excentralizer at the top and an opposing retractable caliper arm at the lower end. The lower housing, which was flexible, contained a transducer at the base, a single receiver 50 cm above the transducer and two button standoffs on the side opposite the caliper arm, one near the transducer, the other near the receiver. When the tool was being lowered, the caliper was retracted but when positioned for a measurement, the caliper was extended, pressing the buttons against the borehole wall. Once the transducer was activated, P-waves were transmitted to the wall through the borehole fluid and S-waves were generated in the borehole wall by P to S conversion. Velocities of both S and P-waves were calculated from transit times measured on photographs of the waveforms.

Figure 3: Lithology vs. estimated depth in the Troodos ophiolite. Bars indicate positions of ICRGD and other drill holes: solid + logged; open + cored only. Abbreviations: UPL, LPL = upper and lower pillow lava; BG = basal group; CUM = cumulate; PYROX. = pyroxenite; BZB = harzburgite; TECT. = tectonite.

Magnetometer.

The total magnetic field was measured using a modified BPB verticality sonde (VO1). This normally consists of three orthogonal fluxgate magnetometers (one vertical, two horizontal) to measure tool azimuth and two inclinometers to measure tilt, in a 2.6 m long x 4.2 cm (1.7") diameter housing. In the present application, the physical configuration remained unchanged but the sensitivity of the fluxgate magnetometers was increased to 50γ so that the tool could function as a borehole magnetometer. Although the total field strength can be calculated as a function of depth from the 3-component fluxgate data, the declination cannot be determined because the tool was not gyro-stabilized. The tool was calibrated before and after each run by measuring the total field at the drillsite with both the borehole sonde and a proton precession magnetometer provided by the Cyprus Geological Survey. Since the borehole magnetometer data obtained in Cyprus is presented in detail elsewhere (Pariso and Johnson, this volume), it will not be discussed further in this paper.

Magnetic susceptibility.

The final tool was a Geoinstruments Ky magnetic susceptibility tool. The probe consisted of a solenoid sensing coil and associated electronics in a 2.5 m long x 5 cm (2") diameter housing. Since the tool only had a pressure rating of 150 bars (the strength of the fiberglass pressure case around the sensor), it could only be lowered to about 1600 m.

Downhole Operations

It was originally intended to log ICRDG holes CY-2, 2a and 4 upon the completion of drilling in CY-4 and then return to log CY-1 and 1a as drilling was completed in CY-1a. This would insure that the most important holes, CY-1a and 4, were logged immediately after drilling while the drill rig was still on site and before the holes had time to collapse. The strategy was successful as far as CY-4 was concerned, but hole CY-1a could not be logged because it tapped a high pressure aquifer and the remaining holes collapsed during or immediately after drilling. For this reason, a series of alternate holes (Table 3) drilled by Hellenic Mining and the Bureau de Recherches Geologiques et Minieres was logged in order to obtain data from sections equivalent to those drilled in holes CY-1, 1a, 2 and 2a (Figure 3).

As can be seen in Table 4, Table 5 and Figure 4, the logging operations themselves were very successful. Over 30.7 km of logs (280K data points) were obtained during the course of 43 separate lowerings in five holes. Nearly 3 km of section representing virtually every lithology in the complex except the ultramafic tectonites was logged, making this the most comprehensive suite of logs ever obtained in oceanic crust.

The deepest hole, CY-4, was logged in two stages: during the first, the interval from 862-2075 m was logged open-hole with all of the logging tools and the interval from 862 m to the surface was logged through the pipe (HQ) using the nuclear (ρ, γ, ϕ) and temperature tools. During the second stage, the interval from 0-640 m was re-logged open-hole with all of the logging tools after the pipe had been pulled. The interval from 640-862 m was never logged open-hole because of stuck pipe and the interval from 2075-2262 m was not logged because it was drilled after the completion of logging. The only difficulty encountered during the logging operations in CY-4 was the loss of the shear wave sonic tool on the last run in the lower part of the hole when the tool became stuck and the cable parted at 1997 m. The tool was successfully fished, however, and the logging run completed, leaving the hole open for further operations.

The logging operations in the alternate holes were completed almost without incident. The only difficulties encountered were an electronic failure in the magnetic susceptibility tool which prevented its use in holes K4, AE4 and M62 and the collapse of hole M62 before it could be logged with the caliper and nuclear tools.

As can be seen in Table 4 and Figure 5, the tools worked well and the hole conditions were optimal for almost all of the tools employed. The water table was close to the surface in all holes and borehole temperatures ranged from 18°C at the surface to a maximum of 45°C at the base of CY-4, or well within the operating limits of the tools. Although the shallow holes at the top of the section (K116, K4, AE4 and M62) were rugose, CY-4 was smooth-walled and all were in gauge (diam. <8") with few cavings. Only two problems were encountered: 1) The resistivity tool saturated intermittently in the lower levels of CY-4 because the formation resistivity exceeded the limits of the tool (80K ohm-m). This occurred because the formation fluid consists of relatively fresh water and the formation itself is tight. 2) The logs obtained between 640-862 m in CY-4 are only intermediate in quality because they were obtained through pipe.

DATA

The logging data obtained in holes K116, K4, AE4, M62 and CY-4 is presented in Figure 6. Only two corrections have been applied: 1) Natural gamma, porosity, density, velocity and resistivity data obtained above the water table and within ±1 m of the breakouts shown in Figure 5 have been deleted. 2) The nuclear logs obtained between 640-862 m in hole CY-4 have been corrected for the pipe by determining the average value for each parameter (natural gamma radiation, porosity, density) in the cased interval, the averages of the data 50 m above and below the casing and correcting the raw data by the differences (+1.5 API units, −7%, and −.14 g/cm^3, respectively).

TABLE 3: Supplementary Drillholes Examined by Logging

Hole[1]	Coordinates	Drilled by	Penetration (m)	Logged Interval (m)	Crustal Level	Lithology	Depth[2] Range (m)
K116	35°00'58"N 33°12'43"E	Hellenic Mining	300	283	Extrusives	Upper pillow basalts Lower pillow basalts	0-50 50-300
K4	34°59'58"N 33°12'15"E	BRGM[3]	116	110	Extrusives	Lower pillow basalts Basal group	0-70 70-116
AE	34°59'42"N 33°07'30"E	BRGM	216	212	Extrusives	Basal group	0-216
M62	35°01'23"N 33°07'05"E	BRGM	208	208	Extrusives Plutonic	Basal group Sheeted dikes	Gradational contact

(1) K = Klirou, AE = Ayios Epiphanious, M = Mitsero;
(2) Based on petrology; (3) BRGM = Bureau de Recherches Geologiques et Minieres.

Although most of the data may be taken at face value and compared directly with oceanic data, the porosity and resistivity data may not, the porosity data because the neutron porosity tool is not calibrated to work in mafic rocks, the resistivity data because the formation is saturated with fresh (actually slightly brackish) water rather than seawater. In consequence, both tools tend to read high.

An accurate porosity log can be calculated from the density log, however, if the grain density, ρ_g, is known as a function of depth, by using the relation:

$$\phi_D = \frac{\rho_g - \rho_{log}}{\rho_g - \rho_f}$$

where ϕ_D is the porosity determined from density, ρ_{log} is the density determined by logging and ρ_f the density of water (1.01 g/cm). In most logging operations, such a log is difficult to reconstruct because of poor recovery, but the ICRDG holes were continuously cored with extremely high recovery (99.9%) and grain densities were determined on core samples every 5 to 10 m (Figure 7). It was thus possible to calculate porosity logs for holes K116, K4, AE4 and CY-4 using the density logs shown in Figure 6 and the average and least squares grain density vs. depth solutions shown in Figure 7. These logs, together with the remaining logs from Figure 6 are presented in Figure 8 after smoothing with a 1000-point (100 m) running average in order to show average formation properties as a function of depth. The shear wave velocities have been smoothed with a 5-point (50 m) running average.

Finally, a synthetic resistivity log was calculated for insitu oceanographic conditions of water saturation and temperature from the calculated porosity log using Archie's Law:

$$R = \frac{R_f}{\phi_D^n}$$

where R is the formation resistivity, n = 2, ϕ_D is the calculated porosity from Equation 1 and R_f is the resistivity of the formation fluid (sea water) calculated from Arp's Law assuming a temperature of 60°C at the sediment/basement contact and a temperature gradient of 100°C/km as in hole 504B (Becker et al., 1985). The resulting log, also shown in Figure 8, was thus calculated on the assumption that the formation resistivity is controlled by porosity and does not take into account second order effects due to surface conduction and metallic minerals.

TABLE 4. Downhole operations summary (supplementary drillholes).

Hole	Run	Date	Logging Interval (m)	Water Table (m)	Logging Direction	Tool/Measurement	Remarks[1]
K116	1	7/2/84	0-283	10	Down	TT1 Temperature	24°C at base of hole
	2	7/2/84	6-283	10	Up	Magnetometer	Not centralized
	3	7/2/84	2-282	10	Up	DD3 Caliper Natural γ γ density	Rugose hole; ave. diameter = 5-3/4"
	4	7/2/84	10-283	10	Up	NN1 Neutron porosity Natural γ	
	5	7/2/84	10-282	10	Up	RO1 Resistivity	
	6	7/2/84	10-282	10	Up	MS1 Vp	
	7	7/2/84	2-282	10	Up	Magnetic susceptibility	
	8	7/2/84	11-280	10	Up	Shear wave sonic	
K4	1	11/6/85	0-111	10	Down	TT1 Temperature	22°C at base of hole
	2	11/6/85	0-111	10	Up	Magnetometer	Not centralized
	3	11/6/85	10-111	10	Up	RO1 Resistivity	
	4	11/6/85	10-110	10	Up	MS1 Vp	Not centralized
	5	11/6/85	20-111	10	Up	Shear wave sonic	
	6	11/7/85	0-110	10	Up	DD3 Caliper Natural γ γ density	Rugose hole; ave. diameter = 5-1/2"
	7	11/7/85	2-111	10	Up	NN1 Neutron porosity Natural γ	
AE4	1	11/9/85	0-213	14	Down	TT1 Temperature	22.5°C at base of hole
	2	11/9/85	17-213	14	Up	RO1 Resistivity	
	3	11/9/85	15-212	14	Up	MS1 Vp	
	4	11/9/85	0-212	14	Up	DD3 Caliper Natural γ γ density	Rugose hole; ave. diameter = 8"
	5	11/9/85	16-213	14	Up	NN1 Neutron porosity Natural γ	
	6	11/9/85	0-213	14	Up	Magnetometer	
	7	11/9/85	20-210	14	Up	Shear wave sonc	
M62	1	11/5/85	1-208	0	Down	TT1 Temperature	22°C at base of hole
	2	11/5/85	1-192	0	Up	Magnetometer	Not centralized
	3	11/5/85	4-191	0	Up	RO1 Resistivity	R_f = 15 ohm/m at 19°C
	4	11/5/85	1-191	0	Up	MS1 Vp	
	5	11/5/85	4-189	0	Up	Shear wave sonic	Rugose hole; ave. diameter = 7-1/2"

(1) Data quality was good in all cases. Holes K116, K4, AE4 and M62 logged open-hole (no casing). Borehole fluid = groundwater.

TABLE 5. Downhole operations summary for CY-4.

Run	Date	Logging Interval (m)	Water Table (m)	Logging Direction	Tool/Measurement	Remarks[1]
1	6/26/84	0-862	80	Down	TT1 Temperature	Inside pipe
		862-2075	80		Temperature	45°C at base of hole
2	6/27/84	0-862	80	Up	DD3 Caliper	Inside pipe
		862-2075	80		Caliper	Smooth hole; diameter = 3-1/4"
		0-862	80		Natural γ	Data Fair. Through pipe
		862-2075	80		Natural γ	
		0-862	80		γ density	Data Fair. Through pipe
		862-2075	80		γ density	
3	6/27/84	864-2075	80	Up	MS1 Vp	Not centralized
4	6/27/84	80-862	80	Up	NN1 Neutron porosity	Through pipe
		862-2075	80		Neutron porosity	
		80-862	80		Natural γ	Data Fair. Through pipe
		862-2075	80		Natural γ	
5	6/28/84	864-2075	80	Up	RO1 Resistivity	R_f = 25 ohm/m at 19°C
6	6/28/– 6/29/84	864-2075	80	Up	Magnetometer	Not centralized
7	6/29/84	864-1580	80	Up	Magnetic susceptibility	Logged to pressure rating of tool
8	6/29/– 6/30/84	863-1997	45	Up	Shear wave sonic	Logged to bridge
9	7/13/84	0-640	45	Down	TT1 Temperature	23°C at base of logged interval
10	7/13/84	0-640	45	Up	DD3 Caliper	Smooth hole; diameter = 4-1/4"
					Natural γ	0-19 m through casing
					γ density	0-19 m through casing
11	7/13/84	46-639	45	Up	MS1 Vp	
12	7/13/84	0-640	45	Up	NN1 Neutron porosity	0-19 m through casing
					Natural γ	
13	7/13/84	20-640	45	Up	Magnetometer	Not centralized
14	7/13/84	46-640	45	Up	RO1 Resistivity	R_f = 20 ohm/m at 18°C
15	7/13/84	20-640	45	Up	Magnetic susceptibility	
16	7/13/84	50-630	45	Up	Shear wave sonic	

(1) Data quality is good accept where indicated. Runs 1-8: logged through casing plus HQ pipe from 0-19 m, through HQ pipe from 19-862 m, open-hole from 862-2075 m. Runs 9-16 logged through casing from 0-19 m, open-hole from 19-640 m. Borehole fluid - mixture of groundwater and Kutwell.

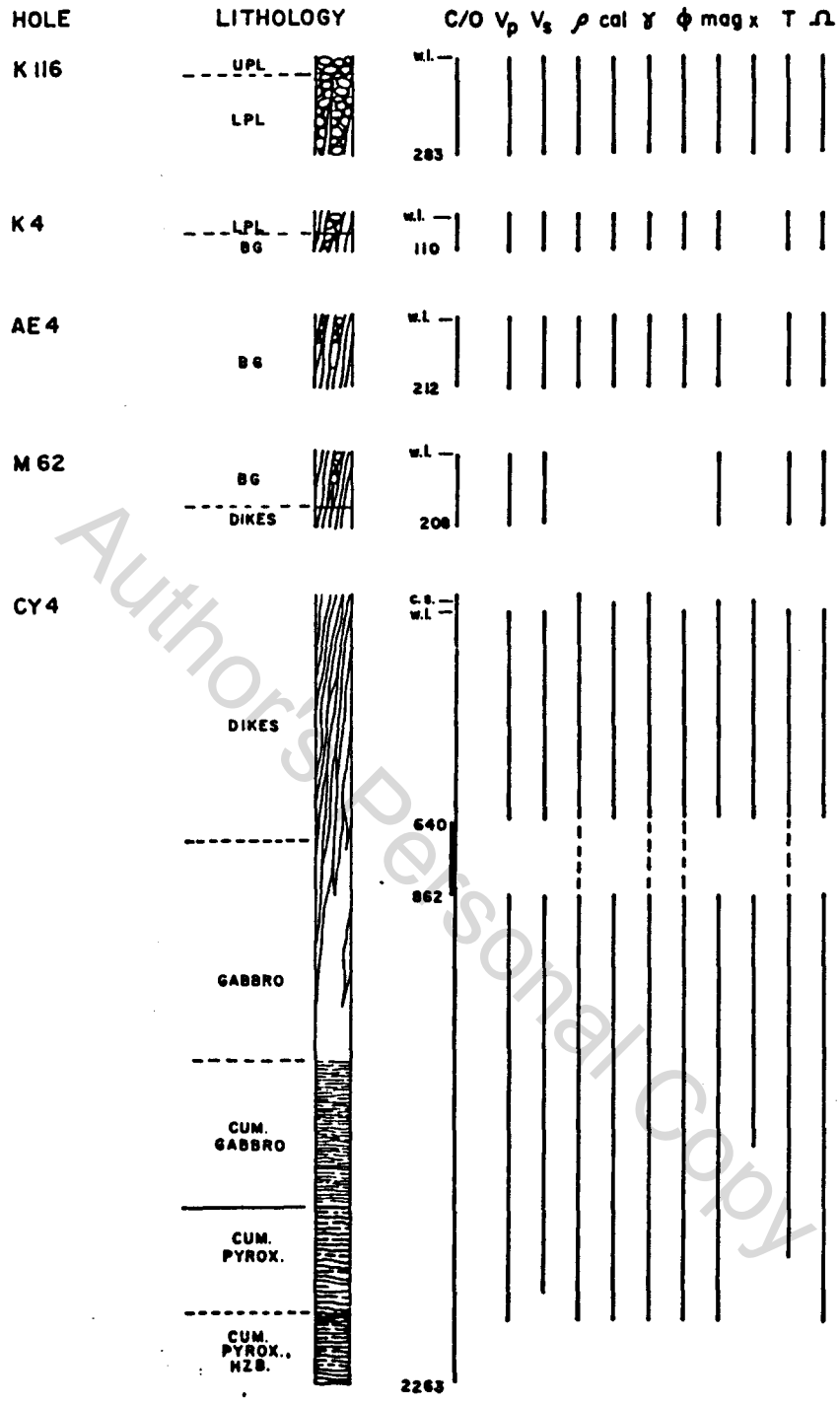

Figure 4: Log quality vs. depth in holes K116, K4, AE4, M62, and CY-4; solid line = good; dashed line = fair; Abbreviations: UPL = upper pillow lava; LPL = lower pillow lava; BG = basal group; CUM = cumulate; HXB = harzburg C/O = cased/open hole; Vp = compressional wave velocity; Vs = shear wave velocity; ρ = density; cal. = caliper; γ = natural gamma radiation; ϕ = neutron porosity; mag. = 3 axis magnetometer; x = magnetic susceptibility; T = temperature; ς = resistivity; w.l. = water level; c.s. = casing shoe. Depth in metres.

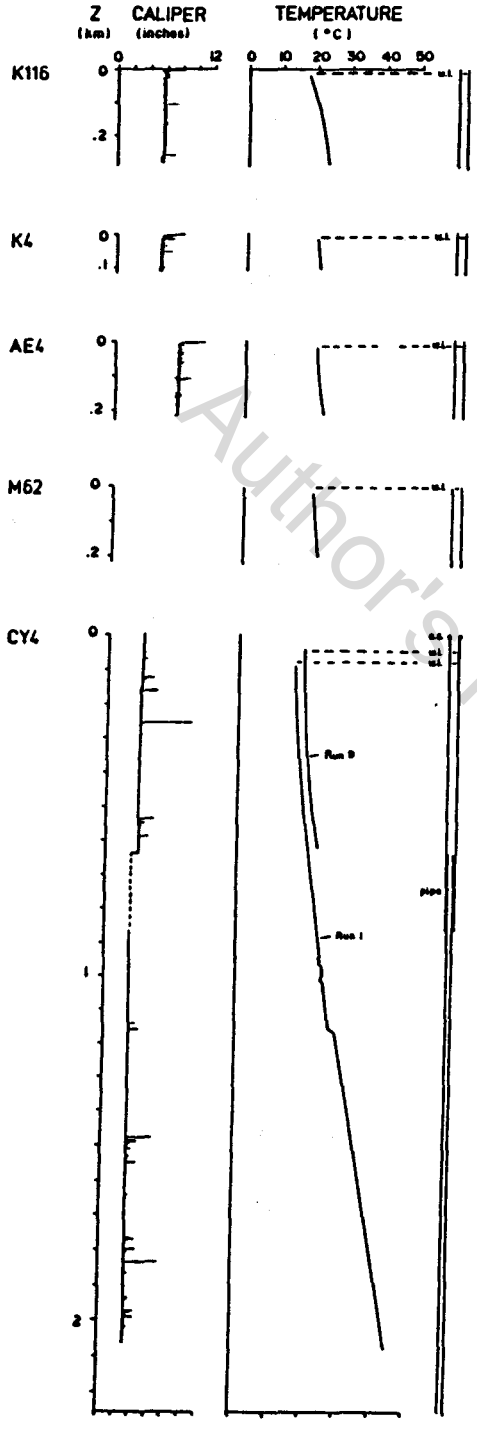

Figure 5: Hole conditions (borehole diameter, temperature) vs. depth in holes K116, K4, AE4, M62 and CY-4. Holes were logged openhole except for interval from 640-862 m in hole CY-4 which was logged through pipe. Abbreviations: w.l. = water level; c.s. = casing shoe

RESULTS

As can be seen in Figures 6 and 8, the geophysical formation properties of the Troodos ophiolite vary markedly with depth in response to changes in porosity and lithology:

Natural gamma radioactivity.

The natural gamma radioactivity of the complex is high and variable (10 to 50 API units about a mean of 30) in the pillow basalts, but decreases irregularly through the pillow basalt/dike transition zone to uniform values of 5-10 API units in the sheeted dikes and finally, to negligible values in the underlying plutonic section. The low natural gamma radioactivity of the plutonic section is typical of fresh rocks of the mafic-ultramafic rock series which normally contain only small amounts of K, U or Th. The higher radioactivity observed in the extrusives is similar to that observed in altered pillow basalts at sea (e.g. DSDP hole 418A; Salisbury et al., in press) where it is associated with K uptake in low temperature alteration products such as K-feldspar, palagonite and other clay minerals (Flower et al., 1980; Holmes, in press). The simultaneous disappearance of dikes and measurable high natural gamma radiation at a depth of 800-900 m in hole CY-4 suggests that sea water penetration in the oceanic crust is controlled by dikes.

Porosity.

As can be seen in Figures 6 and 8 respectively, the apparent and calculated porosities both decrease with depth from a maximum in the pillow basalts to a minimum in the gabbros and ultramafics. Specifically, the calculated porosity curve, which is considered an accurate estimate of the average formation porosity due to cracks, and microcracks, decreases from approximately 20% in the pillow basalts to 5-10% in the sheeted dikes and finally, to 2-4% in the gabbros and negligible values in the ultramafics. The values obtained in the pillow basalts are similar to those obtained at comparable levels in DSDP/ODP holes 418A and 504B (10-20%, and 10-15%, respectively; Becker et al., 1982; Salisbury et al., in press) where packer tests demonstrate that the extrusive section is highly permeable (Anderson and Zoback, 1982). The extremely low porosities measured at deeper levels in the Troodos ophiolite suggest that the intrusive section is tight.

The apparent porosity curve shown in Figure 6 displays the same trend of decreasing porosity with depth as the calculated porosity but invariably gives higher values. This is due to tool calibration problems and the fact that the neutron tool senses bound water as well as water associated with grain boundaries, cracks and interpillow voids. Thus the high apparent porosity in the pillow basalts is likely due to alteration and the slight increase in the ultramafics at the base of the section is probably due to partial serpentinization.

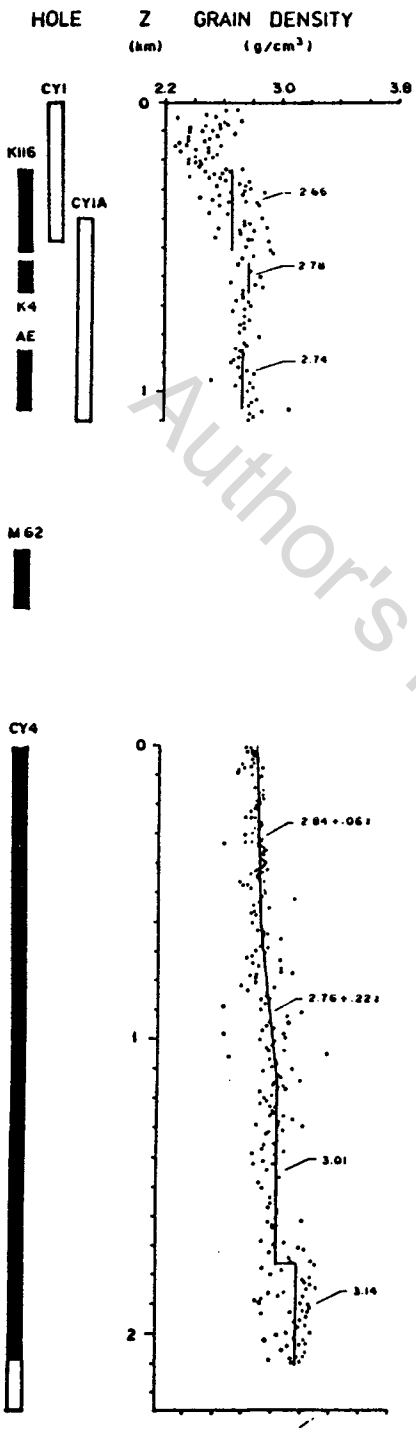

Figure 7: Laboratory grain density data for core samples from holes CY-1, CY-1a and CY-4. Curves represent averages and least squares solutions used to obtain corrected porostiy log.

Density.

As expected, the formation density increases with depth in response to increasing grain density and decreasing porosity. The average density ranges from 2.2-2.3 g/cm^3 in the altered pillow basalts at the top of the section, increases gradually through the pillow basalt/dike transition to values of 2.6-2.8 g/cm^3 in the dikes, increases again to values of 2.9-2.95 g/cm^3 in the gabbros and finally increases abruptly to 3.1 g/cm^3 at the gabbro/pyroxenite boundary. From Figure 8, it is clear that density is controlled largely by porosity since the density varies inversely with porosity. Nonetheless, the sharp increase in density at the top of the pyroxenites is clearly due to a change in composition since both the apparent and the calculated porosity show little change across the gabbro/pyroxenite boundary while the average grain density jumps by 0.13 g/cm^3 (Figure 7). It is also apparent from Figure 7 that the increase in formation density observed from the pillow basalts to the base of the gabbros is due in part to a gradual increase in grain density which we attribute, in turn, to decreasing alteration and glass content with depth.

Velocity.

Perhaps the most striking logs obtained in the Troodos ophiolite are the compressional and shear wave velocity logs. These show that Vp and Vs are low and fairly uniform in the pillow basalts (3.2-3.5 and 2.0-2.2 km/s, respectively), but increase irregularly through the pillow basalt/dike transition to values as high as 5.0 and 3.0 km/s, respectively, near the base of the transition zone (Basal Group). Within the sheeted dikes, velocities continue to increase irregularly with depth in response to increasing metamorphic grade (Christensen and Salisbury, this volume) and eventually, to the presence of gabbro screens. Near the base of the dikes, where the gabbro screens and dikes are about equally abundant (600 m in hole CY-4), Vp increases rapidly to 6.4 km/s and then more slowly through the remainder of the dike/gabbro transition to uniform values of 6.7-6.9 km/s in the gabbros, while Vs rises to 3.5 km/s in the transition and ranges between 3.2-3.5 km/s in the gabbros. In the deepest unit logged, the pyroxenites, Vp reaches values as high as 7.4 km/s but averages 7.0, while Vs averages 4.0 km/s. Since pyroxenites are often fast parallel to layering, however, and the logging tool only measures velocity in the vertical direction, the average compressional wave velocities reported here may be low.

As in the case of density, the velocity of the section is controlled largely by formation porosity and only secondarily by composition except in the gabbros and ultramafics where the porosity is negligible. Thus the formation velocities are generally lower than the measured velocities of rocks from equivalent depths (Smith and Vine, 1987; Christensen et al., 1987; Christensen and Salisbury, 1989).

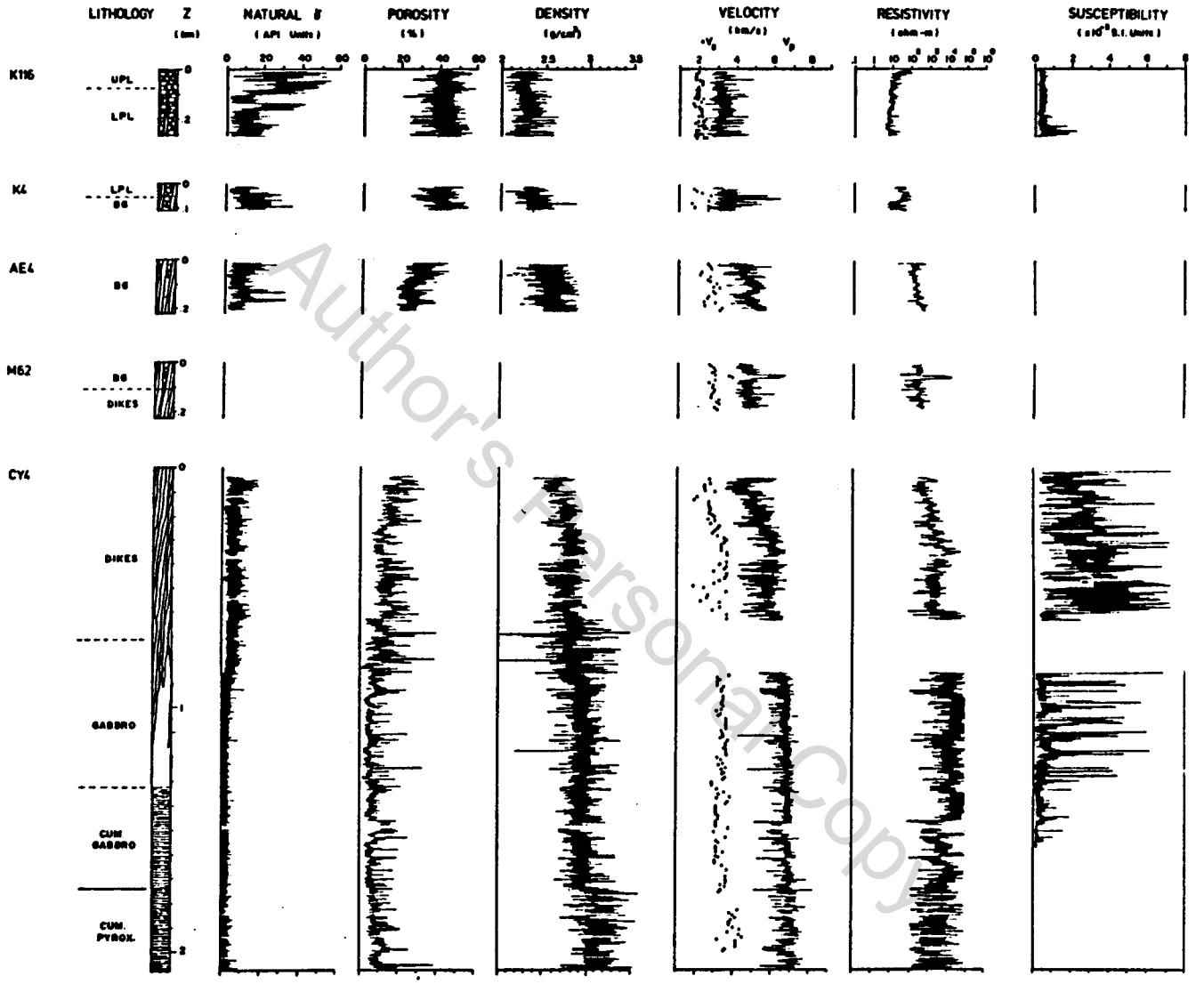

Figure 6: Natural gamma, apparent porosity, density, velocity (Vp and Vs), resistivity and susceptibility logging data from holes K116, K4, AE4, M62 and CY-4. Data from breakouts (see Figure 5) has been deleted and data from cased interval between 640-862 m has been corrected for pipe. Abbreviations as in Figure 4.

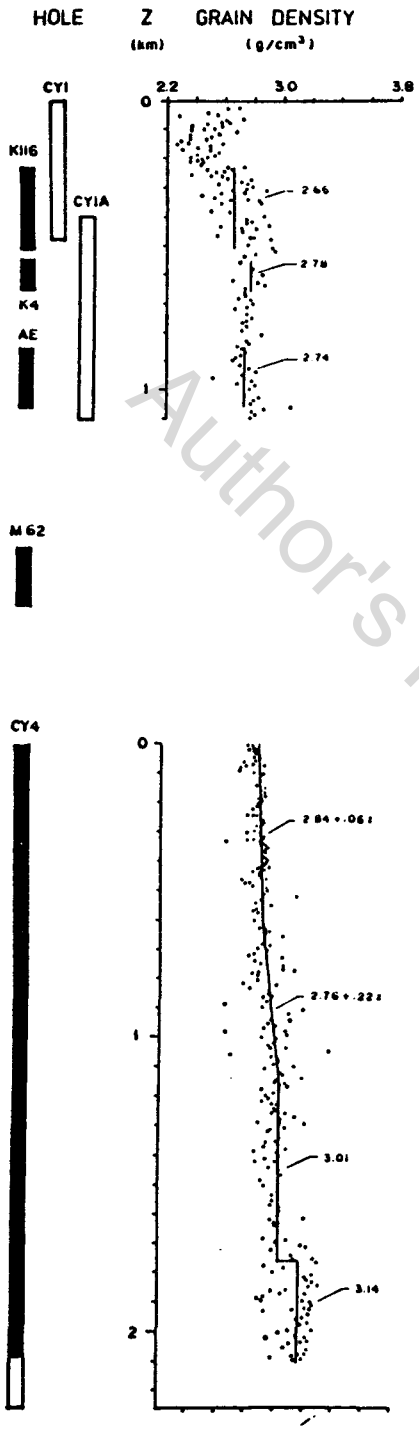

Figure 7: Laboratory grain density data for core samples from holes CY-1, CY-1a and CY-4. Curves represent averages and least squares solutions used to obtain corrected porostiy log.

Density.

As expected, the formation density increases with depth in response to increasing grain density and decreasing porosity. The average density ranges from 2.2-2.3 g/cm^3 in the altered pillow basalts at the top of the section, increases gradually through the pillow basalt/dike transition to values of 2.6-2.8 g/cm^3 in the dikes, increases again to values of 2.9-2.95 g/cm^3 in the gabbros and finally increases abruptly to 3.1 g/cm^3 at the gabbro/pyroxenite boundary. From Figure 8, it is clear that density is controlled largely by porosity since the density varies inversely with porosity. Nonetheless, the sharp increase in density at the top of the pyroxenites is clearly due to a change in composition since both the apparent and the calculated porosity show little change across the gabbro/pyroxenite boundary while the average grain density jumps by 0.13 g/cm^3 (Figure 7). It is also apparent from Figure 7 that the increase in formation density observed from the pillow basalts to the base of the gabbros is due in part to a gradual increase in grain density which we attribute, in turn, to decreasing alteration and glass content with depth.

Velocity.

Perhaps the most striking logs obtained in the Troodos ophiolite are the compressional and shear wave velocity logs. These show that Vp and Vs are low and fairly uniform in the pillow basalts (3.2-3.5 and 2.0-2.2 km/s, respectively), but increase irregularly through the pillow basalt/dike transition to values as high as 5.0 and 3.0 km/s, respectively, near the base of the transition zone (Basal Group). Within the sheeted dikes, velocities continue to increase irregularly with depth in response to increasing metamorphic grade (Christensen and Salisbury, this volume) and eventually, to the presence of gabbro screens. Near the base of the dikes, where the gabbro screens and dikes are about equally abundant (600 m in hole CY-4), Vp increases rapidly to 6.4 km/s and then more slowly through the remainder of the dike/gabbro transition to uniform values of 6.7-6.9 km/s in the gabbros, while Vs rises to 3.5 km/s in the transition and ranges between 3.2-3.5 km/s in the gabbros. In the deepest unit logged, the pyroxenites, Vp reaches values as high as 7.4 km/s but averages 7.0, while Vs averages 4.0 km/s. Since pyroxenites are often fast parallel to layering, however, and the logging tool only measures velocity in the vertical direction, the average compressional wave velocities reported here may be low.

As in the case of density, the velocity of the section is controlled largely by formation porosity and only secondarily by composition except in the gabbros and ultramafics where the porosity is negligible. Thus the formation velocities are generally lower than the measured velocities of rocks from equivalent depths (Smith and Vine, 1987; Christensen et al., 1987; Christensen and Salisbury, 1989).

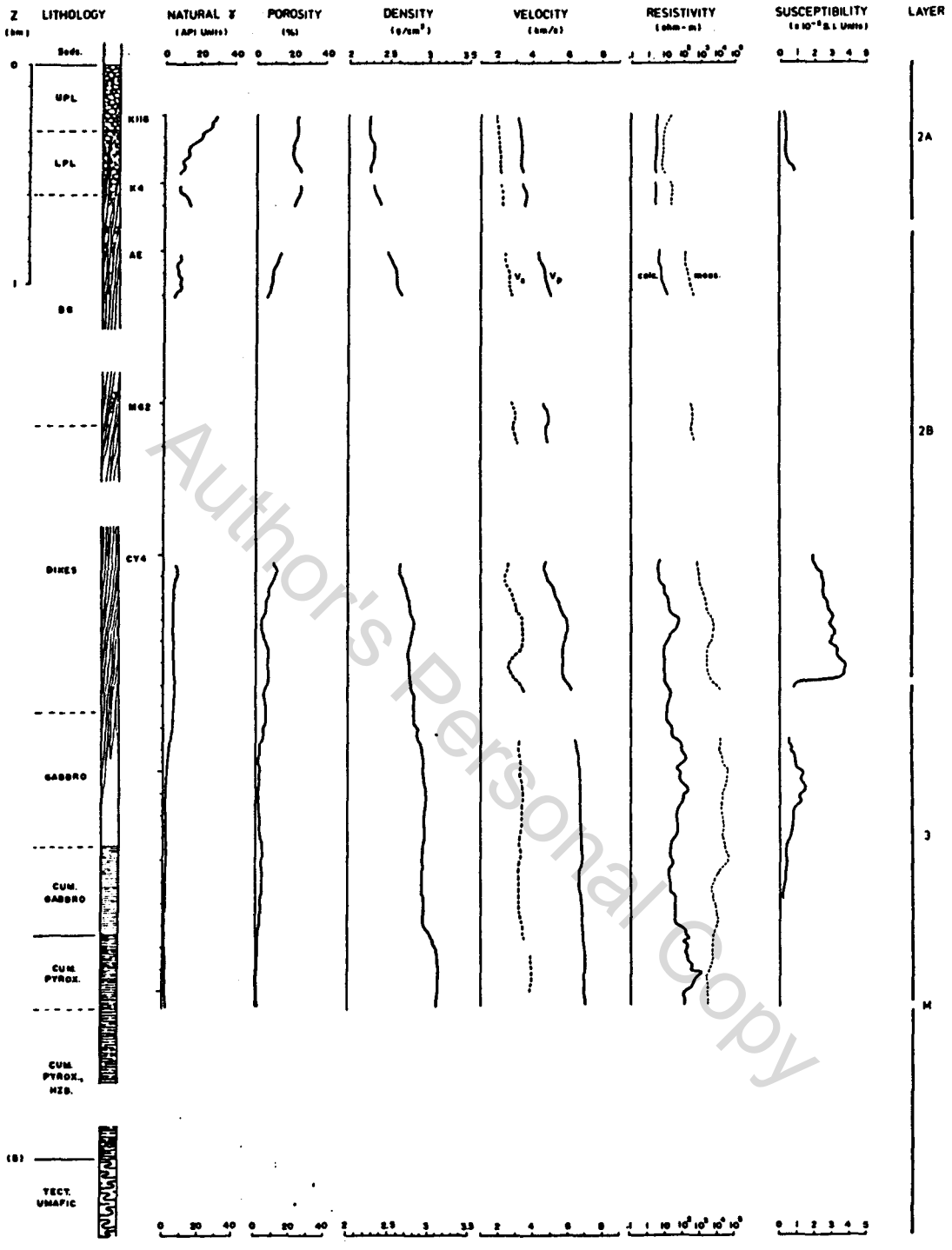

Figure 8: Average formation properties vs. depth and lithology in the Troodos ophiolite. Porosity log calculted for density log and measured grain densities; calculated resistivity log derived from calculated porosity log assuming cracks and pores are filled with seawater, T = 60°C at the sediment/basement contact and a geothermal gradient of 100°C/km as in DSDP hole 504B. Equivalent oceanic velocity layers are shown on right

Nonetheless, the velocity logs obtained in the Troodos ophiolite agree quite well with the limited suite of logs obtained to date in equivalent sections at sea. The compressional wave velocities obtained in DSDP/ODP hole 504B, for example, increase from approximately 3.5 km/s in the pillow basalts to 6.0 km/s in the sheeted dikes, while Vs increases from about 2.0 km/s to 3.2 km/s over the same interval (Newmark et al., 1985). Similarly, the compressional wave velocities logged in the only extensive interval of submarine gabbros drilled to date average 6.5-6.7 km/s (ODP hole 735; P.T. Robinson, personal communication) and would undoubtedly be higher at confining pressures equivalent to those logged in the Troodos Massif (the gabbros in hole 735 are exposed on the seafloor and are thus at a low effective confining pressure).

Resistivity.

As can be seen in Figures 6 and 8, the measured resistivity increases irregularly from a low of about 10 ohm-m in the pillow basalts to approximately 2000 ohm-m near the base of the dikes. At the dike/gabbro boundary defined above (50% dikes, 50% gabbro screens), the resistivity increases sharply by an order of magnitude and ranges between 20K-50K ohm-m in the massive gabbros before decreasing again in the cumulate gabbros and ultramafics to values as low as 3000 ohm-m. While the measured values shown in Figures 6 and 8 may be high compared to oceanic values since the formation fluid consists of brackish, rather than sea water, the trends would appear to be correct: resistivities are low in the pillow basalts due to high porosity and surface conduction in clays and other alteration products; the resistivity increases markedly with depth in response to decreasing porosity; near the bottom of the section, the resistivity decreases again due to mineral conduction in magnetite and to surface conduction in serpentine minerals.

The calculated resistivity is invariably lower than the measured resistivity since it takes into account the presence of sea water and assumes an oceanic geothermal gradient. While the two curves mimic each other throughout the dikes, the trend is less convincing in the pillow basalts at the top of the section and in the cumulate gabbros and ultramafics at the base. It is likely, however, that if mineral and surface conduction effects, were also taken into account, the calculated values would be lower in these intervals and the match would improve. Although resistivity logs have not been obtained in oceanic crust to the depths logged in Cyprus, where logs have been obtained in equivalent lithologies, the trends and values have been similar. For example, the resistivities increase with depth by more than an order of magnitude in the uppermost kilometer of hole 504B and range from 5-30 ohm-m in the pillow basalts to between 100-500 ohm-m in the sheeted dikes (Becker, 1985).

TABLE 6: Ocean Crust Layered Velocity Models.

Layer	Velocity Vp (km/s)	Thickness (km)
Raitt (1963)		
2	5.07 ± 0.63	1.71 ± 0.75
3	6.69 ± 0.26	4.86 ± 1.42
Mantle	8.13 ± 0.24	–
Peterson et al. (1974)		
1	1.7–2.0	0.5
2A	2.5–3.8	0.5–1.5
2B	4.0–6.0	0.5–1.5
3A	6.5–6.8	2.0–3.0
3B	7.0–7.8	2.0–5.0
Mantle	8.1	–
Houtz and Ewing (1976 Pacific case)		
2A	3.33 ± 0.10	0.74 ± 0.23
2B	5.23 ± 0.44	0.72 ± 0.26
2C	6.19 ± 0.16	1.83 ± 0.75(1)
3	6.92 ± 0.17	–(2)

(1) Cumulative thickness of Layers 2B and 2C.
(2) In general, the mantle and Layer 3 were not detected.

Magnetic Susceptibility.

The final, and perhaps most distinctive, log obtained in the Troodos ophiolite is the magnetic susceptibility log. As can be seen in Figures 6 and 8, the susceptibility is very low (less than 0.5×10^{-3} S.I. Units) in the pillow basalts but rises with increasing magnetite content through the sheeted dikes to an average of about 4×10^{-3} S.I. Units near the dike/gabbro transition at 600 m in hole CY-4. In the underlying gabbros, magnetite disappears and the susceptibility decreases abruptly to about 0.5×10^{-3} S.I. Units , with higher spikes marking individual dikes cutting the gabbro. Although not shown in these figures, the susceptibility values in the sheeted dikes display a bimodal distribution which suggests the presence of at least two generations of dikes.

CONCLUSIONS

It has been suggested that the ophiolites are fragments of oceanic crust which have been emplaced on land by tectonic processes and subsequently exposed by erosion. While attractive and accepted by most geologists, the hypothesis has been difficult to prove: Drilling in the ocean basins has failed to recover a complete section through the crust for comparison with the ophiolites. Dredging in oceanic transforms has recovered lithologies similar to those observed in ophiolites, but the crust is thin and sheared in the vicinity of transforms and was produced in an anomalous thermal environment (e.g., Mutter et al., 1984). Similarly, geophysical studies in the ophiolites have not been entirely successful in reconstructing the geophysical properties of the ophiolites for comparison with oceanic data: while recent refraction studies in the Troodos extrusives give velocities consistent with those of Layer 2 (Eleftheriou and Schoenharting, 1987), velocities characteristic of Layer 3 have not been detected deeper in the section (Khan et al., 1972). Similarly, laboratory studies of the velocities of samples from ophiolites tend to give maximum velocities, especially in the upper parts of the section, because they fail to take cracks into consideration (e.g. Salisbury and Christensen, 1978).

The insitu logging data obtained in the Troodos ophiolite, on the other hand, is in excellent agreement with logging data obtained in the upper levels of the oceanic crust and with the geophysical properties of the lower crust inferred from marine geophysical studies. From this fact, and the data presented in Figures 6 and 8, we conclude that:

1. In geophysical terms, the Troodos ophiolite is almost indistinguishable from oceanic crust. However, the Oceanic Layer (Layer 3) is thin, even though the total thickness of the crust falls within the range of thicknesses observed at sea (Table 5). This is consistent with formation near an oceanic fracture zone such as the Arakapas Fault.

2. From a comparison of velocity logs and petrology in the Troodos Massif, Layer 2A consists of pillow basalts, 2B consists of the pillow basalt to dike transition plus the underlying sheeted dikes, and Layer 3 consists of massive gabbros, cumulate gabbros and pyroxenites. If the section was restored to full pressure, the velocity of the sheeted dikes would almost certainly rise to those of Layer 2C as defined by Houtz and Ewing (1976) and the velocities of the pyroxenites would match those of Layer 3B or even the uppermost mantle, if measured in the horizontal direction. The harzburgites were not logged, but from laboratory studies of the velocities of samples from this interval (Christensen and Salisbury, this volume) it is clear they will display mantle velocities (7.8-8.1 km/s) since the formation porosity approaches zero.

3. The Layer 2/3 boundary marks the transition from sheeted dikes to massive gabbros and represents not only a velocity discontinuity, but a pronounced resistivity discontinuity (plus 10×) and a sharp magnetic susceptibility discontinuity (minus 5×).

4. Throughout the upper levels of the crust, most formation properties are controlled largely by porosity, which decreases dramatically with depth from a maximum of about 20% in the pillow basalts to negligible values at the base of the dike/gabbro transition. Thus the density, velocity and resistivity are all low and relatively uniform in the pillow basalts of Layer 2A but increase irregularly throughout Layer 2B in response to decreasing porosity.

5. Below the dike/gabbro transition, the formation properties are controlled by composition and approach rock properties. This implies that the lower oceanic crust is impermeable.

6. It follows that circulation involving sea water penetrates no deeper than the base of the dike/gabbro transition. This is confirmed by the absence of K-bearing clays at greater depths and demonstrates that except in anormalous regions such as fracture zones, rock-seawater interaction is limited to the upper levels of the crust.

ACKNOWLEDGEMENTS

We wish to thank Ken Lowe, Peter Mackowiak and Paul Stedman of B.P.B. Instruments for their assistance in obtaining the logs, Dr. Andreas Panayiotou and the Staff of the Geological Survey Department, Cyprus, for their excellent logistical support, Dr. James Hall and Lata Hall for their encouragement and considerable assistance in the field and the International Crustal Research Drilling Group for the opportunity to participate in the project. We also wish to thank Jane Barrett for typing the manuscript and Mel Best for serving as a reviewer. This work was supported under NSF grant EAR 82-18096, ONR contract N84K0207 and NSERC grant 0039133.

REFERENCES

Anderson, R.N. and Zoback, M.D.
1982: Permeability, under-pressures and convection in the oceanic crust near the Costa Rica Rift, eastern equatorial Pacific; Journal of Geophysical Research, v. 87, p. 2860-2868.

Becker, K.
1985: Large-scale electrical resistivity and bulk porosity of the oceanic crust, Deep Sea Drilling Project Hole 504B, Costa Rica Rift; *in* Initial Reports of the Deep Sea Drilling Project, R.N. Anderson, J. Honnorez, K. Becker, et al.; U.S. Government Printing Office, Washington, D.C., v. 83, p. 419-428.

Becker, K., Langseth, M.G., Von Herzen, R.P., Anderson, R.N. and Hobart, M.A.
1985: Deep crustal geothermal measurements, Hole 504B, Deep Sea Drilling Project, Legs 69, 70, 83 and 92; *in* Initial Reports of the Deep Sea Drilling Project, R.N. Anderson, J. Honnorez, K. Becker, et al.; U.S. Goverment Printing Office, Washington, D.C. v. 83 p. 405-418.

Becker, K., Von Herzen, R.P., Francis, T.J.G., Anderson, R.N., Honnorez, J., Adamson, A.C., Alt, J.C., Emmermann, R., Kempton, P.D., Kinoshita, H., Laverne, C., Mottl, M.J. and Newmark, R.L.
1982: In situ electrical resistivity and bulk porosity of the oceanic crust, Costa Rica Rift; Nature, v. 300, p. 594-598.

Christensen, N.I., Wepfer, W.W. and Salisbury, M.H.
1987: Seismic properties of samples from the volcanic section of the Troodos ophiolite, Hole CY-2a; *in* Cyprus Crustal Study Project Initial Report, Holes CY2-2a, ed. P.T. Robinson, I.L. Gibson and A. Panayiotou; Geological Survey of Canada, Paper 85-29, p. 307-316.

Christensen, N.I. and Salisbury, M.H.
1989: Velocity structure of the Troodos Massif, an arc-derived ophiolite; *in* Cyprus Crustal Study Project Initial Report, Hole CY-4, ed. I.L. Gibson, J. Malpas, P.T. Robinson and C. Xenophontos; Geological Survey of Canada, Paper 88-9.

Coleman, R.G.
1977: Ophiolites: Ancient Oceanic Lithosphere?; Springer-Verlag, Berlin; Heidelberg; New York.

Eleftheriou, S. and Schoenharting, G.
1987: A seismic survey at the Agrokipia mine, Cyprus: the velocity structure of a hydrothermally altered extrusive section of the Troodos ophiolite; *in* Cyprus Crustal Study Project Initial Report Holes CY2-2a, ed. P.T. Robinson, I.L. Gibson and A. Panayiotou; Geological Survey of Canada, Paper 85- 29, p. 317-326.

Flower, M., Ohnmacht, W., Robinson, P., Marriner, G. and Schminke, H.-U.
1980: Lithologic and chemical stratigraphy at Deep Sea Drilling Project Sites 417 and 418; *in* Initial Reports of the Deep Sea Drilling Project, Part 2, ed. T. Donnelly, J. Francheteau, W. Bryan, P. Robinson, M. Flower, M. Salisbury, et al.; U.S. Government Printing Office, Washington, D.C., v. 51, 52, 53, p. 939-956.

Gass, I.G.
1968: Is the Troodos Massif of Cyprus a fragment of Mesozoic ocean floor?; Nature, v. 220, p. 39-42.

Gillis, K.M.
1986: Multistage alteration of the extrusive sequence, Troodos ophiolite, Cyprus; unpublished Ph.D. Thesis, Dalhousie University, Halifax, Nova Scotia, Canada, 387 p.

Holmes, M.A.
In Press: Evidence for continuous and discontinuous alteration in DSDP Hole 418A basalts and its significance to natural gamma ray log readings; *in* Proceedings of the Ocean Drilling Program Initial Reports, ed. M.H. Salisbury, J.H. Scott, et al.; Part B, v. 102

Houtz, R. and Ewing, J.
1976: Upper crustal structure as a function of plate age; Journal of Geophysical Research, v. 81, p. 2490-2498.

Khan, M.A., Summers, C., Bamford, S.A.D., Chroston, P.N., Poster, C.K. and Vine, F.J.
1972: Reversed seismic refraction line on the Troodos Massif, Cyprus; Nature, v. 238, p. 134-136.

Miyashiro, A.
1973: The Troodos ophiolite complex was probably formed in an island arc; Earth and Planetary Science Letters, v. 19, no. 2, p. 218-224.

Moores, E.M. and Vine, F.J.
1971: Troodos Massif Cyprus, and other ophiolites as oceanic crust: evaluation and implications; *in* A discussion on the Petrology of Igneous and Metamorphic Rocks from the Ocean Floor; Philosophical Transactions of the Royal Society of London, Series A, v. 268, p. 443-466.

Mutter, J.C., Detrick, R.S. and NAT Study Group,
1984: Multichannel seismic evidence for anomalously thin crust at oceanic fracture zones; Geology, v. 12, p. 534-537.

Newmark, R.L., Anderson, R.N., Moos, D. and Zoback, M.D.
1985: Sonic and ultrasonic logging of Hole 504B and its implications for the structure, porosity and stress regime of the upper 1 km of the oceanic crust; *in* Initial Reports of the Deep Sea Drilling Project, R.N. Anderson, J. Honnorez, K. Becker, et al.; U.S. Government Printing Office, Washington, D.C., v. 83, p. 479-510.

Pariso, J. and Johnson, H.P.
1989: Magnetic properties of an analog of the lower oceanic crust: Magnetic logging and paleomagnetic measurements from drill hole CY-4 in the Troodos ophiolite; *in* Cyprus Crustal Study Project: Initial Report, Hole CY-4, ed. I.L.

Magnetic Susceptibility.

The final, and perhaps most distinctive, log obtained in the Troodos ophiolite is the magnetic susceptibility log. As can be seen in Figures 6 and 8, the susceptibility is very low (less than 0.5×10^{-3} S.I. Units) in the pillow basalts but rises with increasing magnetite content through the sheeted dikes to an average of about 4×10^{-3} S.I. Units near the dike/gabbro transition at 600 m in hole CY-4. In the underlying gabbros, magnetite disappears and the susceptibility decreases abruptly to about 0.5×10^{-3} S.I. Units , with higher spikes marking individual dikes cutting the gabbro. Although not shown in these figures, the susceptibility values in the sheeted dikes display a bimodal distribution which suggests the presence of at least two generations of dikes.

CONCLUSIONS

It has been suggested that the ophiolites are fragments of oceanic crust which have been emplaced on land by tectonic processes and subsequently exposed by erosion. While attractive and accepted by most geologists, the hypothesis has been difficult to prove: Drilling in the ocean basins has failed to recover a complete section through the crust for comparison with the ophiolites. Dredging in oceanic transforms has recovered lithologies similar to those observed in ophiolites, but the crust is thin and sheared in the vicinity of transforms and was produced in an anomalous thermal environment (e.g., Mutter et al., 1984). Similarly, geophysical studies in the ophiolites have not been entirely successful in reconstructing the geophysical properties of the ophiolites for comparison with oceanic data: while recent refraction studies in the Troodos extrusives give velocities consistent with those of Layer 2 (Eleftheriou and Schoenharting, 1987), velocities characteristic of Layer 3 have not been detected deeper in the section (Khan et al., 1972). Similarly, laboratory studies of the velocities of samples from ophiolites tend to give maximum velocities, especially in the upper parts of the section, because they fail to take cracks into consideration (e.g. Salisbury and Christensen, 1978).

The insitu logging data obtained in the Troodos ophiolite, on the other hand, is in excellent agreement with logging data obtained in the upper levels of the oceanic crust and with the geophysical properties of the lower crust inferred from marine geophysical studies. From this fact, and the data presented in Figures 6 and 8, we conclude that:

1. In geophysical terms, the Troodos ophiolite is almost indistinguishable from oceanic crust. However, the Oceanic Layer (Layer 3) is thin, even though the total thickness of the crust falls within the range of thicknesses observed at sea (Table 5). This is consistent with formation near an oceanic fracture zone such as the Arakapas Fault.

2. From a comparison of velocity logs and petrology in the Troodos Massif, Layer 2A consists of pillow basalts, 2B consists of the pillow basalt to dike transition plus the underlying sheeted dikes, and Layer 3 consists of massive gabbros, cumulate gabbros and pyroxenites. If the section was restored to full pressure, the velocity of the sheeted dikes would almost certainly rise to those of Layer 2C as defined by Houtz and Ewing (1976) and the velocities of the pyroxenites would match those of Layer 3B or even the uppermost mantle, if measured in the horizontal direction. The harzburgites were not logged, but from laboratory studies of the velocities of samples from this interval (Christensen and Salisbury, this volume) it is clear they will display mantle velocities (7.8-8.1 km/s) since the formation porosity approaches zero.

3. The Layer 2/3 boundary marks the transition from sheeted dikes to massive gabbros and represents not only a velocity discontinuity, but a pronounced resistivity discontinuity (plus 10×) and a sharp magnetic susceptibility discontinuity (minus 5×).

4. Throughout the upper levels of the crust, most formation properties are controlled largely by porosity, which decreases dramatically with depth from a maximum of about 20% in the pillow basalts to negligible values at the base of the dike/gabbro transition. Thus the density, velocity and resistivity are all low and relatively uniform in the pillow basalts of Layer 2A but increase irregularly throughout Layer 2B in response to decreasing porosity.

5. Below the dike/gabbro transition, the formation properties are controlled by composition and approach rock properties. This implies that the lower oceanic crust is impermeable.

6. It follows that circulation involving sea water penetrates no deeper than the base of the dike/gabbro transition. This is confirmed by the absence of K-bearing clays at greater depths and demonstrates that except in anormalous regions such as fracture zones, rock-seawater interaction is limited to the upper levels of the crust.

ACKNOWLEDGEMENTS

We wish to thank Ken Lowe, Peter Mackowiak and Paul Stedman of B.P.B. Instruments for their assistance in obtaining the logs, Dr. Andreas Panayiotou and the Staff of the Geological Survey Department, Cyprus, for their excellent logistical support, Dr. James Hall and Lata Hall for their encouragement and considerable assistance in the field and the International Crustal Research Drilling Group for the opportunity to participate in the project. We also wish to thank Jane Barrett for typing the manuscript and Mel Best for serving as a reviewer. This work was supported under NSF grant EAR 82-18096, ONR contract N84K0207 and NSERC grant 0039133.